

Electrochemical Studies of 2-amino-1, 9-dihydro-9-((2-hydroxyethoxy) methyl)-6H-purin-6-one as Green Corrosion Inhibitor for Mild Steel in 1.0 M Hydrochloric Acid Solution

Chandrabhan Verma¹, M.A. Quraishi^{1,*}, E.E. Ebenso²

¹Department of Applied Chemistry, Indian Institute of Technology, Banaras Hindu University, Varanasi-221005, India

²Material Science Innovation & Modelling (MaSIM) Research Focus Area, Faculty of Agriculture, Science and Technology, North-West University (Mafikeng Campus), Private Bag X2046, Mmabatho 2735, South Africa

*E-mail: maquraishi.apc@itbhu.ac.in

Received: 9 March 2013 / Accepted: 5 April 2013 / Published: 1 May 2013

The influence of Acyclovir (2-amin-1,9-dihydro-9-((2-hydroxyethoxy)methyl)-6H-purin-6-one) on the corrosion rate of Mild Steel in 1.0 M HCl was investigated by gravimetric and electrochemical methods. It was found that the Acyclovir acts as an efficient corrosion inhibitor for mild steel in 1.0 M HCl. The inhibition efficiency increases with increasing the inhibitor concentration. The maximum efficiency was found to be 92% at 500ppm concentration. The adsorption of Acyclovir drug on the mild Steel surface follows the Langmuir adsorption isotherm. The electrochemical results indicated that the investigated compound acts as mixed-type inhibitor. Some thermodynamic parameters were also determined to investigate the mechanism of corrosion inhibition.

Keywords: Kinetic parameters; Mild steel; EIS; Acid corrosion

1. INTRODUCTION

Chemical inhibitors play an important role in the protection of various metals from corrosion [1]. Most of the commercial inhibitors are toxic in nature. Thus there is need for development of environmentally inhibitors. [2-3]. Drugs and plant extracts [4-9] seem to be ideal candidates to replace traditional toxic chemicals inhibitors. The literature survey reveals that following drugs were used as efficient corrosion inhibitors for mild steel corrosion in acidic solutions: Ceftriaxone, Cefalexin, Doxycycline, Pheniramine, Fexofenadine, Cefotaxime, Cefuroxime, Cefapirin, Dapsone,

Mebendazole, Penicillin G, Penicillin V, Cefadroxil, Ampicillin, Sparfloxacin, Chloramphenicol, Ketoconazole, Methocarbamol, Orphenadrine, Cefotaxime, Cefazolin and Metformin [10-31].

In present work, we have studied corrosion inhibition of Acyclovir on corrosion of mild steel in 1 M HCl using gravimetric and electrochemical methods. Acyclovir is manufactured by Cipla Pharma Limited. The IUPAC name of the drug is 2-Amino-1,9-dihydro-9-((2-hydroxyethoxy)methyl)-6H-purin-6-one. Its structure is given in Figure 1. Its molecular formula is $C_8H_{11}N_5O_3$ and Molecular mass is 225.21 g/mol. The LD50 dose of Acyclovir is 20000 mg/kg for Rat.

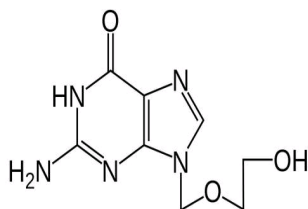


Figure 1. Structure of Acyclovir ((2-amin-1,9-dihydro-9-((2-hydroxyethoxy)methyl)-6H-purin-6-one)

2. EXPERIMENTAL

2.1 Materials

The mild steel specimens, with composition (wt %) Fe 99.30%, C 0.076%, Si 0.026%, Mn 0.192%, P 0.012%, Cr 0.050%, Ni 0.050%, Al 0.023%, and Cu 0.135%, were abraded successively with emery papers from 600 to 1200 mesh/in grade then washed with double distilled water, rinsed in acetone and finally dried. After drying, the specimens were placed in desiccators and then used. All experiments were carried out in unstirred solutions of 1M HCl which was prepared by dilution of analytical grade HCl (37%) with double distilled water. The specimens having area $2.5 \times 2.0 \times 0.025$ cm³ were used for weight loss experiments and electrochemical measurements were carried out on a 7.5 cm long stem with exposed area of 1.0×1.0 cm² and remaining portion were covered with epoxy resin.

2.2 Test Solution

Stock solutions of Acyclovir were made by dissolving it in 1 M HCl solution and for dilution double distilled water was used.

2.3 Weight loss method

The weight loss measurements were performed by immersing the mild steel coupons in 100ml of 1 M HCl in conical flasks in absence and in presence of different concentrations of inhibitor. After the elapsed time, the mild steel specimen were taken out, washed, dried and weighed accurately. All

the experiments were performed in triplicate in aerated 1M HCl and average values were taken. The corrosion inhibition efficiency (η %) and surface coverage (θ) is calculated by following equations:

$$\eta \% = \frac{C_R - C_{R(i)}}{C_R} \times 100 \quad (1)$$

$$\theta = \frac{C_R - C_{R(i)}}{C_R} \quad (2)$$

where C_R and $C_{R(i)}$ are the corrosion rate values in absence and presence of inhibitor respectively.

The corrosion rate (CR) of mild steel in acidic medium was calculated by using the relation:

$$C_R = \frac{W}{A t} \quad (3)$$

where W is weight loss of mild steel (mg), A is the area of the coupon (cm^2), t is the exposure time(h). [32]

2.4 Electrochemical impedance spectroscopy

The impedance behavior of mild steel in the presence and in absence of inhibitor was studied using three electrode assembly at 308K temperature. The mild steel (working electrode), saturated calomel electrode (reference electrode) and platinum foil (counter electrode). The Gamry instrument Potentiostat/Galvanostat having a Gamry framework system based on ESA 400 in a frequency range of 10^{-2} Hz to 10^5 Hz under Potentiodynamic conditions, with amplitude of 10 mV peak-to-peak, using AC signal at E_{corr} . Gamry applications include software DC105 for corrosion and EIS 300 for EIS measurements, and Echem Analyst version 5.50 software packages for data fitting.

From charge transfer resistance the corrosion inhibition efficiency (η %) of Acyclovir is calculated by following equation:

$$\eta(\%) = \frac{R_{\text{ct}}' - R_{\text{ct}}^0}{R_{\text{ct}}'} \times 100 \quad (4)$$

where, R_{ct}^i and R_{ct}^0 are the charge transfer resistance in presence and absence of inhibitor, respectively.

2.5 Potentiodynamic polarization

The electrochemical corrosion behavior of mild steel in the presence and absence of inhibitor was studied by recording the anodic and cathodic potentiodynamic polarization curves at 308K

temperature. The measurements were performed in 1 M HCl using different concentration of inhibitor by automatically changing the electrode potential between ± 250 mV versus OCP at a scan rate of 1 mV s^{-1} . The electrochemical parameters such as corrosion current densities (i_{corr}) derived from extrapolating the anodic and cathodic linear segment of Tafel Polarization curves and efficiency was calculated by using following equation.

$$\eta (\%) = \frac{i_{\text{corr}}^0 - i'_{\text{corr}}}{i_{\text{corr}}^0} \times 100 \quad (6)$$

where, i_{corr}^0 and i'_{corr} are the corrosion current density in absence and presence and absence of inhibitor, respectively.

2.6 Linear polarization measurement

The Linear Polarization behavior of mild steel in 1M HCl in absence and presence of different concentration of inhibitor was studied at ± 20 mV versus OCP at a scan rate of 0.125 mV s^{-1} . The polarization resistance (R_p) was calculated from the slope of curve in vicinity of corrosion potential and corrosion inhibition efficiency ($\eta\%$) was calculated by using following equation:

$$\eta \% = \frac{R_p^i - R_p^0}{R_p^i} \times 100 \quad (7)$$

where R_p^i and R_p^0 and are polarization resistance in inhibited and uninhibited solutions respectively.

3. RESULTS AND DISCUSSION

3.1 Weight loss measurements

3.1.1. Effect of inhibitor concentration

Weight loss measurements were carried out using different concentrations of inhibitor. The weight loss, inhibition efficiency and corrosion rate are reported in the Table1. It is observed that the inhibition efficiency increases with increase in concentration of inhibitor up to 500 ppm and further increase in concentration does not show any appreciable rise in inhibition efficiency. The inhibitor showed a maximum efficiency of 92.6% in HCl at an optimum concentration of 500 ppm. Figure 2(a) shows that inhibition efficiency ($\eta\%$) and the degree of surface coverage (θ) increase with increasing concentration of inhibitor.

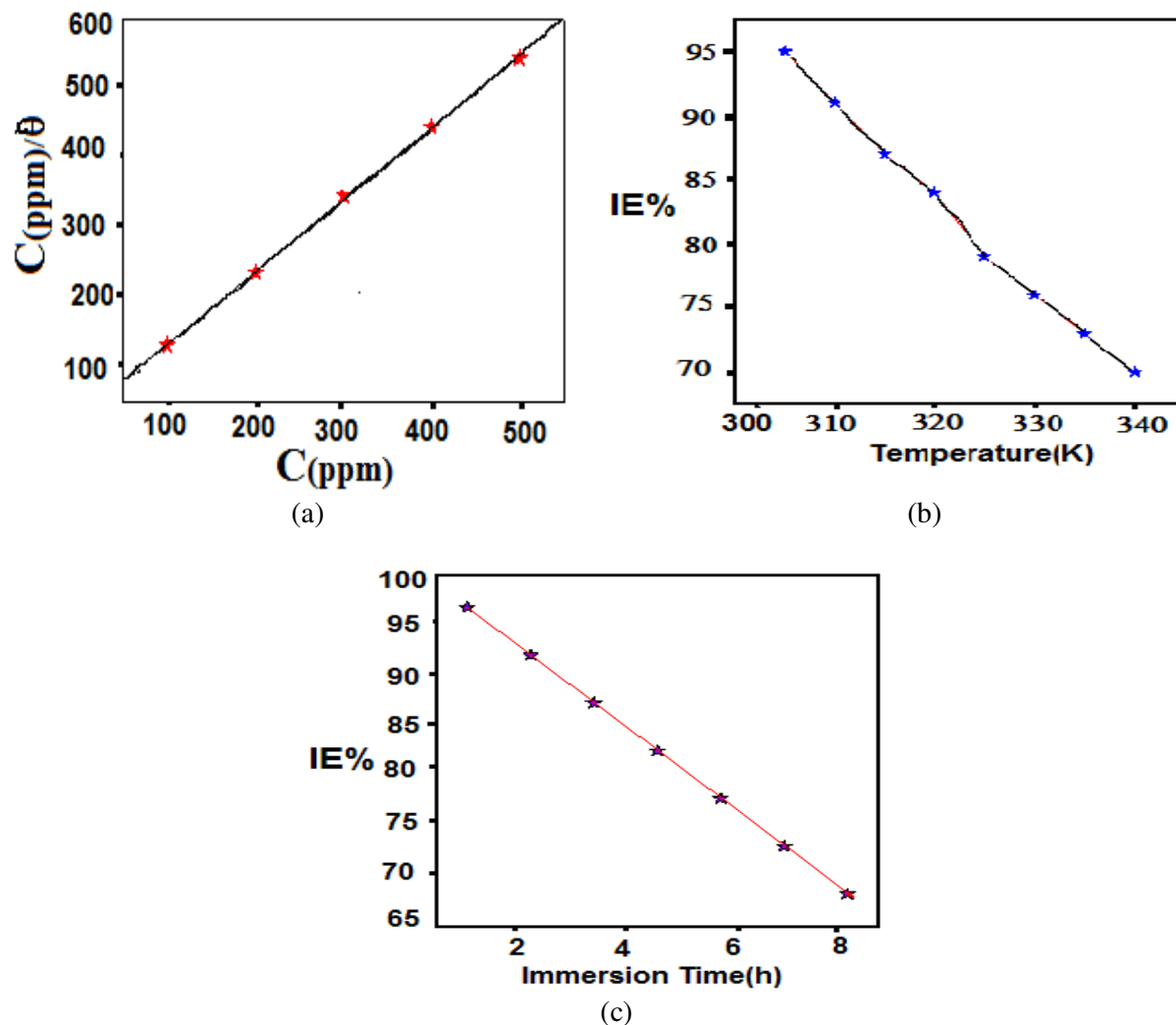


Figure 2. (a) Inhibition efficiency of Acyclovir at different concentrations (b) Inhibition efficiency of Acyclovir at different temperatures (c) Inhibition efficiency of Acyclovir at different immersion times

Table 1. Corrosion rate and Inhibition efficiency ($\eta\%$) for the mild steel in 1 M HCl in the absence and in the presence of different concentration of inhibitor.

Inhibitor	Concentration (ppm)	Surface coverage (θ)	$\eta\%$	CR (mmy^{-1})
Acyclovir	Blank	-	-	164
	100	0.776	77.6	37
	200	0.868	85.8	23
	300	0.872	87.2	21
	400	0.904	90.4	16
	500	0.926	92.6	12

3.1.2. Effect of Temperature

The effect of temperature on inhibition efficiency was also studied. It is clear from Figure 2 (b) that on increasing temperature from 305 to 340 K inhibition efficiency decreases from 92 to 70 %. The decrease in inhibition efficiency with temperature attributed indicate desorption of inhibitor from mild steel surface. This observation is attributable to an increased rate of dissolution process of mild steel and partial desorption of the inhibitor from the metal surface with increasing temperature.

3.1.3. Effect of Immersion time

In order to assess the stability of inhibitive behavior on a time scale, Weight loss measurements were performed in 1 M HCl in absence and presence of inhibitor for 1 to 8 h of immersion time. Effect of immersion time versus inhibition efficiency graph was shown in Figure 2(c). It is observed that on increasing immersion time from 1 to 8 h efficiency decreases from 92 to 72 %. This shows that with increasing immersion time, desorption process of inhibitor is facilitated leading to a decrease in inhibition efficiency.

3.1.4 Thermodynamic activation parameters

The corrosion rate depends upon temperature; this temperature dependency is given by Arrhenius equation and transition state equation:

$$\log(C_R) = \frac{-E_a}{2.303RT} + \log \lambda \quad (8)$$

$$C_R = \frac{RT}{Nh} \exp\left(\frac{\Delta S^*}{R}\right) \exp\left(-\frac{\Delta H^*}{RT}\right) \quad (9)$$

Where E_a apparent activation energy, λ is the pre-exponential factor, ΔH^* is the apparent enthalpy of activation, ΔS^* the apparent entropy of activation, h Planck's constant and N is the Avogadro number.

The apparent Activation energy (E_a) of the Blank acid solution and inhibitor are given in to the Table (2). From the table it is observed that the, value of activation energy of inhibitor is greater than the free acid solution. This show that corrosion rate of mild steel is mainly controlled by activation energy.

The linear plot between $\log(CR)$ vs. $1/T$ and $\log(CR/T)$ vs. $1/T$ were performed. As shown in Figure 2(a) straight line obtained with a slope $-\Delta E_a/2.303R$, $-\Delta H^*/2.303R$ and an intercept of $[\log(R/Nh) + (\Delta S^*/2.303R)]$, from which values of E_a , ΔH^* and ΔS^* were calculated and given in Table 2:

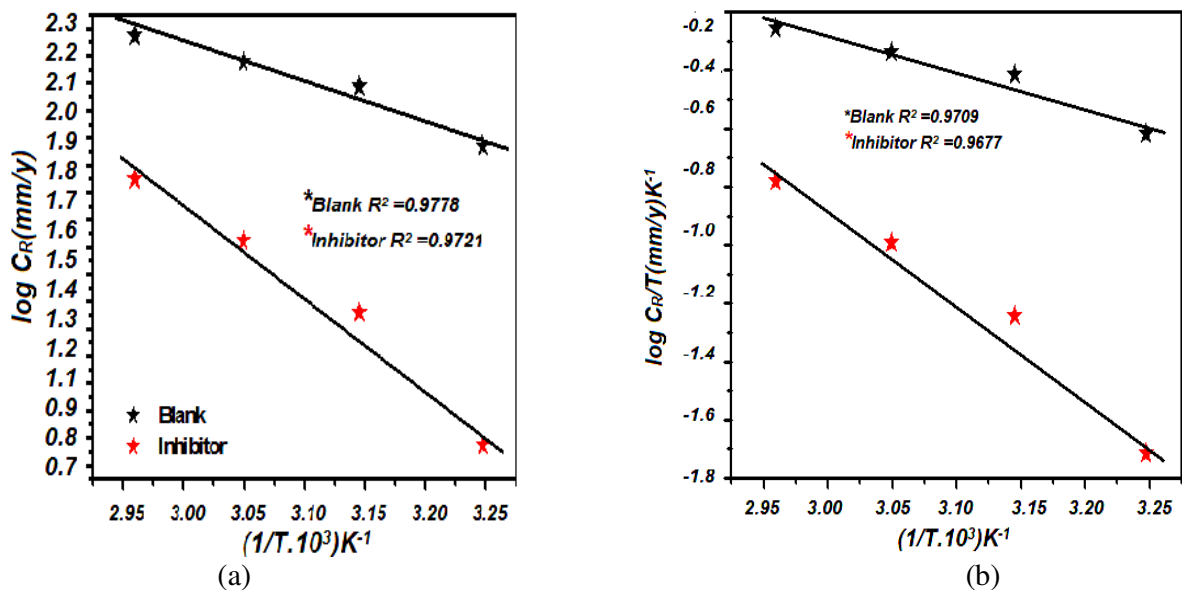


Figure 3. (a) Arrhenius plots of log CR versus 1/T (b) Transition state plots of log CR/T versus 1/T

Table 2. Thermodynamic parameter for mild steel in 1M HCl in absence and presence of optimum concentration of inhibitor:

Inhibitor	E_a (kJ mol ⁻¹)	$-\Delta G_{ads}$ (kJ mol ⁻¹)				K_{ads} (M ⁻¹ 10 ³)				ΔH (kJ mol ⁻¹)	ΔS (JK ⁻¹ mol ⁻¹)
		308	318	328	338	308	318	328	338		
Blank	23.48	--	--	--	--	--	--	--	--	21.04	-178.9
Acyclovir	63.35	-34.6	-33.8	-33.6	-32.3	13.6	6.4	4.04	1.79	22.90	-97.2

3.1.4 Thermodynamic parameters and adsorption isotherm

The adsorption isotherms give information about the nature and mechanism of adsorption of inhibitor molecules. The Langmuir adsorption isotherm can be expressed by following equation.

$$\frac{C_{(inh)}}{\theta} = \frac{1}{K_{(ads)}} + C_{(inh)} \quad (10)$$

where, $C_{(inh)}$ is inhibitor concentration and K_{ads} is equilibrium constant for adsorption-desorption process. The value of θ increases with increasing the concentration of inhibitor and decreases with increasing temperature. Various isotherm plots were tested. The best result was obtained from Langmuir isotherm Figure 4(a).

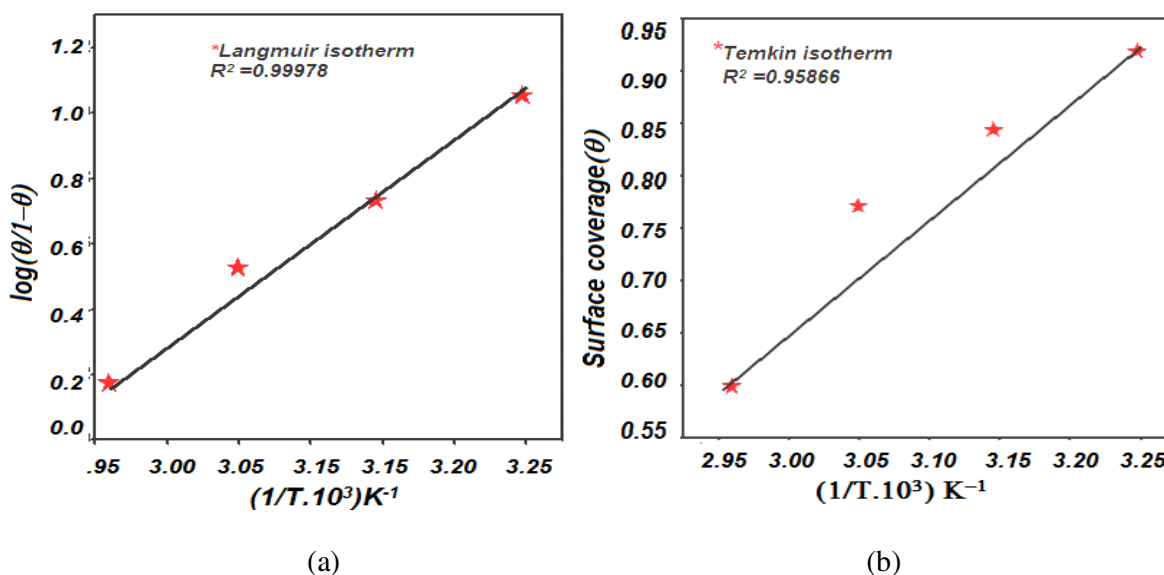


Figure 4. (a) Langmuir adsorption isotherm (b) Temkin adsorption isotherm

The plot between $\log(\theta/(1-\theta))$ and $1/T$ is shown in Figure 4(a). The value of heat of adsorption was determined from the slope ($-\Delta G_{ads}/2.303RT$) of the graph. The free energy (ΔG_{ads}) of adsorption and adsorption constant (K_{ads}) were calculated by following equations:

$$\Delta G_{ads}^{\circ} = -RT \ln(55.5K_{ads}) \quad (11)$$

$$\ln K_{ads} = \frac{-\Delta H_{ads}^{\circ}}{RT} + \text{constant} \quad (12)$$

The negative sign of free energy of adsorption shows that adsorption of Acyclovir on mild steel is a spontaneous process and it also shows the strong interaction between inhibitor and mild steel [33]. The value of ΔG_{ads} in case of Acyclovir is found to be around -32 kJ mol^{-1} , showing that Acyclovir is adsorbed by mixed mode of adsorption which involves both physical and chemical adsorption [34].

3.2.1 Electrochemical impedance spectroscopy

The impedance behavior of mild steel in 1M HCl in absence and presence of different concentration of Acyclovir is shown as Nyquist plot in Figure 5(a) and EIS parameter such as R_s , Y_0 , R_{ct} , and C_{dl} were derived from the Nyquist plot are given in Table 4. Equivalent circuit shown in Figure 5(b) was used to analyze impedance data. The double layer capacitance (C_{dl}) was calculated by using the following equation [35]:

$$C_{dl} = Y_0 (\omega_{max})^{n-1} \quad (13)$$

where Y_0 is CPE coefficient, n is CPE exponent (phase shift), ω is the angular frequency. The ω_{max} represents the frequency at which the imaginary component reaches a maximum. It is the frequency at which the real part (Z_r) is midway between the low and high frequency x-axis intercepts

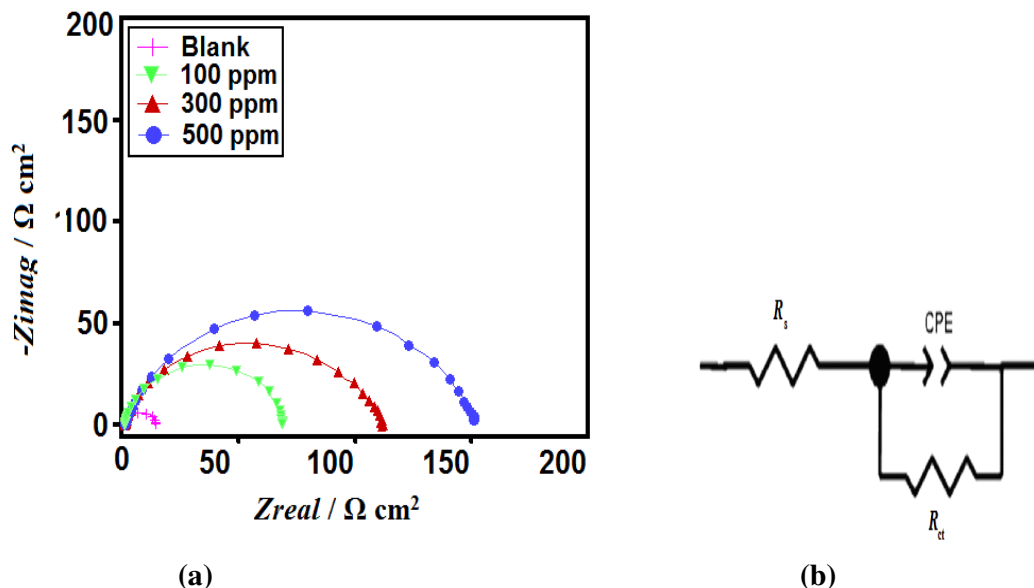


Figure 5. (a) Nyquist plots in absence and presence of different concentrations of Inhibitor. (b) Equivalent circuit used to fit the impedance data.

It is clear from the result that value of R_{ct} increases from 11.8/ Ω cm² (Blank) to 148.5/ Ω cm² on addition of 500ppm of inhibitor .The value of C_{dl} decreases from 138.2μF cm⁻² (Blank) to 47.76 μF cm⁻²). The decrease in capacitance (C_{dl}) on addition of inhibitor may be due to increase in local dielectric constant and/or may be due to increase in the thickness of the double layer, showing that Acyclovir inhibited Iron metal corrosion in by adsorbing at metal/acid interfaces [36].

Table 3. The Electrochemical Impedance and Linear polarization parameters and corresponding efficiencies of Acyclovir in 1.0 M HCl at different concentration

Inhibitor	Conc. (ppm)	EIS data						Linear Polarization data	
		R_s (Ω cm ²)	Y_0 (10 ⁻⁶ Ω ⁻¹ cm ⁻²)	n	R_{ct} (Ω cm ²)	C_{dl} (μF cm ⁻²)	$\eta\%$	R_p	$\eta\%$
Acyclovir	Blank	0.909	482.2	0.808	11.82	138.22	-	13.93	-
	100	0.914	89.8	0.901	67.96	48.26	81.9	83.61	84.2
	300	1.057	52.15	0.888	106.94	27.93	88.5	101.1	86.98
	500	1.420	64.81	0.852	148.5	27.10	91.7	146	90.98

The Amplitudes of CPE was calculated by using following equation:

$$Z_{\text{CPE}} = \left(\frac{1}{Y_0} \right) [(j\omega)_n]^{-1} \quad (14)$$

where Y_0 is magnitude of CPE , j is an imaginary constant. The value of n (phase shift) it gives information about degree of inhomogeneity.

3.2.2 Linear polarization measurement:

The inhibition behavior of Acyclovir in 1 M HCl in presence and absence of different concentration of inhibitor were also calculated Linear polarization parameters given in Table 3. The efficiency found by Linear polarization shows good agreement to efficiency obtained from Tafel and EIS that data.

3.2.3 Potentiodynamic Polarization measurements

The Potentiodynamic Polarization behavior of mild steel in 1M HCl in absence and in presence of different concentration of Acyclovir is shown as Tafel plot in Figure 6. The various Electrochemical Potentiodynamic parameters such as corrosion potential (E_{corr}), corrosion current density (I_{corr}), anodic and cathodic slope (β_a and β_c) were calculated from Tafel plots are given in Table (4): It is seen that addition of Acyclovir decreases the corrosion current (I_{corr}) density from 3750 $\mu\text{A}/\text{cm}^2$ (Blank) to 85.8 $\mu\text{A}/\text{cm}^2$ thereby giving the efficiency of 92% at the 500 ppm concentration.

Table 4. The Potentiodynamic polarization data of mild steel in 1M HCl in absence and in different concentration of Acyclovir.

Inhibitor Conc(ppm)	Potentiodynamic polarization Parameter				
	$-E_{\text{corr}}$ (mV vs. SCE)	I_{corr} ($\mu\text{A cm}^{-2}$)	β_a (mV d^1)	β_c (mV d^1)	$\eta\%$
Blank	495	3750	89.9	152.9	
100	467	229	80.3	179.1	79
300	472	161	75.8	113.7	85
500	453	85.8	47.6	77.6	92

The addition of inhibitor did not cause significant shift of E_{corr} . The maximum shift was 42 mV towards noble direction thus investigated compound behaves as mixed type of inhibitor. Table 4 shows that inhibition efficiency increases with increasing the concentration of inhibitor.

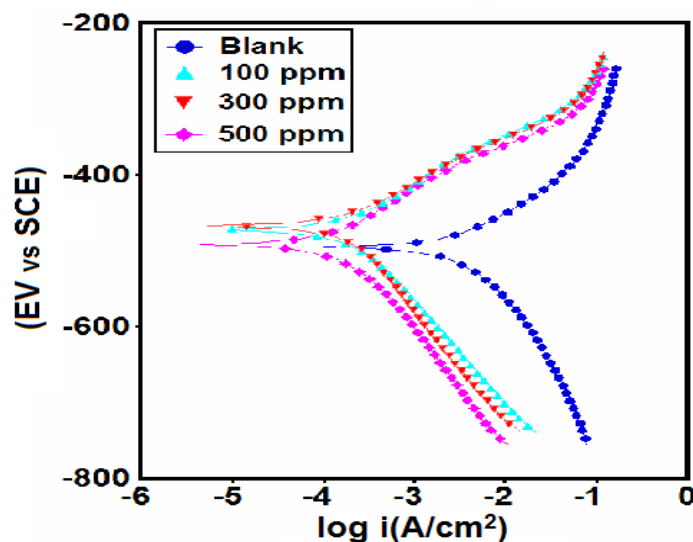


Figure 6. Tafel polarization curves for corrosion of mild steel in 1.0 M HCl in the absence and presence of different concentrations of Acyclovir.

4. MECHANISM OF CORROSION INHIBITION

Corrosion inhibition of mild steel in 1M HCl by Acyclovir can be explained on the basis of molecular adsorption of inhibitor on to the mild steel surface. It is generally considered that the first step in the corrosion inhibition of a metal is the adsorption of the inhibitor molecules at metal / solution interface [37].

Thus Acyclovir can adsorb on the mild steel surface by following ways:

- (a) Electrostatic interaction between the charged molecules and charged metal;
- (b) Interaction of π -electrons with the metal;
- (c) Interaction of unshared pair of electrons in the molecule with the metal; and
- (d) The combination of the all the effects [38,39].

5. CONCLUSIONS

From above study it is concluded that:

1. The Acyclovir (2-amin-1,9-dihydro-9-((2-hydroxyethoxy)methyl)-6H-purin-6-one) is a good inhibitor for corrosion of mild steel in 1M HCl solution. The maximum efficiency was found to be 92% at 500ppm concentration.
2. The adsorption of Acyclovir on mild steel surface obeyed the Langmuir isotherm.
3. The Potentiodynamic studies revealed that Acyclovir is a mixed type inhibitor i.e. it affected both cathodic and anodic reactions.

4. The negative values of ΔG shows that adsorption of Acyclovir on mild steel is a spontaneous process.

References

1. R. Hausler, Corrosion Inhibition and inhibitors, in: G.R. Brubaker, P.B.P. Phipps(Eds.), Corrosion Chemistry, ACS Symposium Series, American Chemical Society, Washington, DC, 1979, p. 262.
2. G. Broussard, O. Bramantit, F.M. Marchese, *O Occup. Med.* 47 (1997) 337–340.
3. P.B. Raja, M.G. Sethuraman, *Mater. Lett.* 62 (2008) 113–116.
4. D.J. Newman, G.M. Cragg, K.M. Snader, *J. Nat. Prod.* 66 (2003) 1022–1037.
5. D.J. Newman, G.M. Cragg, *J. Nat. Prod.* 70 (2007) 461–477.
6. A.L. Harvey, *Drug Discov. Today* 13 (2008)894–901.
7. S. Struck, U. Schmidt, B. Gruening, I.S. Jaeger, J. Hossbach, R. Preissner, *Genome Inform.* 20 (2008) 231–242.
8. O.V. Enick, Do pharmaceutically active compounds have an ecological impact, M.Sc. Thesis, Simon Fraser University, Burnaby, 2006
9. L.R. Chauhan, G. Gunasekaran, *Corros. Sci.* 49 (2007) 1143–1161
10. M.A. Quraishi and S. K. Shukla. *Journal of Appl. Electrochem.* 39 (2009), 1517.
11. S. K. Shukla and M. A. Quraishi, *Mater. Chem. Phys.* 120 (2010) 142.
12. S. K. Shukla and M. A. Quraishi, *Corros. Sci.* 52 (2010) 314.
13. I. Ahamad, R. Prasad and M. A. Quraishi, *Corros. Sci.* 52 (2010) 3033.
14. I. Ahamad, R. Prasad and M. A. Quraishi, *Journal of Solid State Electrochem.* 14 (2010) 2095.
15. A. K. Singh and M. A. Quraishi. *Journal of Applied Electrochem.* 41 (2011) 7.
16. A.K. Singh, M. A. Quraishi and Eno E. Ebenso, *Int. J. Electrochem. Sci.*, 6 (2011) 5676.
17. A.K. Singh, Eno E. Ebenso and M. A. Quraishi, *Int. J. Electrochem. Sci.* 7 (2012) 2320.
18. A. Singh, A. K. Singh and M. A. Quraishi, *The Open Electrochem. J.* 2 (2010) 43.
19. I. Ahamad and M. A. Quraishi, *Corros. Sci.* 52, (2010), 651.
20. N. O. Eddy, S. A. Odoemelam and P. Ekwumemgbo, *Sci. Res. Essays* 4 (2009) 33.
21. N. O. Eddy and S. A. Odoemelam, *Adv. Nat. Appl. Sci.* 2 (2008) 225.
22. S. K. Shukla, M. A. Quraishi and Eno E. Ebenso, *Int. J. Electrochem. Sci.* 6 (2011) 2912.
23. N. O. Eddy, Eno E. Ebenso and U. J. Ibok, *J. Appl. Electrochem.* 40 (2010) 445.
24. S. K. Shukla, Eno E. Ebenso and M. A. Quraishi, *Int. J. Electrochem. Sci.* 6 (2011) 2912.
25. N. O. Eddy, S. R. Stoyanov, Eno E. Ebenso, *Int. J. Electrochem. Sci.* 5 (2010) 1127.
26. N. O. Eddy, U. J. Ibok, Eno E. Ebenso, A. El Nemr and E.S.H. El Ashry, *J. Mol. Mod.* 15 (2009) 1085.
27. I. B. Obot, *Port. Electrochim. Acta.* 27 (2009) 539.
28. Eno E. Ebenso, N. O. Eddy and A. O. Odiongenyi, *Port. Electrochim. Acta.* 27 (2009) 13.
29. S. K. Shukla and M. A. Quraishi, *Corros. Sci.* 51 (2009) 1007.
30. A. K. Singh and M. A. Quraishi, *Corros. Sci.* 52 (2010) 152.
31. A. Singh, E. E. Ebenso, M. A. Quraishi, *Int. J. Electrochem. Sci.*, 7 (2012) 4766 - 4779
32. M. G. Fontana, *Corrosion Engineering*, Mcgrawhill, Singapore, (1987) 173.
33. F. Zucchi, G. Trabaneli and G. Brunoro, *Corros. Sci.* 33 (1992) 1135.
34. K.F. Khaled, *Electrochim. Acta* 53 (2008) 3492
35. C. S. Hsu and F. Mansfeld, *Corrosion.* 57 (2001) 747
36. R.A. Prabhu, T.V. Venkatesha, A.V. Shanbhag, G.M. Kulkarni, R.G. Kalkhambkar, *Corros. Sci.* 50 (2008) 3356–3362.
37. M. Sahin, S. Bilgic, H. Yilmaz, *Appl. Surf. Sci.* 195 (2002) 1.

38. H. Shorky, M. Yuasa, I. Sekine, R.M. Issa, H.Y. El-Baradie, G.K. Gomma, *Corros. Sci.* 40 (1998) 2173.
39. D.P. Schweinsberg, G.A. George, A.K. Nanayakkara, D.A. Steiner, *Corros. Sci.* 28 (1988) 33.

© 2013 by ESG (www.electrochemsci.org)